

## HYBRID SCHEMES FOR EULER EQUATIONS IN LAGRANGIAN COORDINATES \*

PAVEL BUREŠ AND RICHARD LISKA.

**Abstract.** Many fluid dynamics problems modeled by Euler equations involve large changes of volume or size of computational domain or moving boundaries and thus have to be treated in moving Lagrangian coordinates. Composite schemes are defined by global composition of Lax-Wendroff (LW) and Lax-Friedrichs (LF) schemes. The hybrid methods extend composite schemes in the way, that the combination of the LW and LF scheme is done locally in the form of an affine combination of its numerical fluxes with a local shock switch which guarantees second order accuracy on smooth solutions. Hybrid schemes are developed in 1D and 2D. Numerical results of several test problems are presented.

**Key words.** Euler equations, hybrid method, composite schemes, Lax-Wendroff scheme, Lax-Friedrichs scheme, Lagrangian coordinates

**AMS subject classifications.** 65M06, 76N15

**1. Introduction.** Many hydrodynamical problems described by the Euler equations involve large dynamical changes of computational area or moving boundaries and cannot be treated on static Eulerian computational mesh. Typical problems of this kind coming from laser plasma physics are corona expansion or target compression. Such problems have to be treated in Lagrangian coordinates on computational mesh moving with the fluid. Standard numerical methods for Euler equations in Lagrangian coordinates [10] discretize scalar quantities (density, internal energy and pressure) in cells and velocities in nodes. For treating shock waves appearing in the solution of Euler equations these methods employ artificial viscosity. The choice of the artificial viscosity is however quite a difficult issue [2]. Artificial viscosity is a term that is smoothing solution in the areas of discontinuities. Another approach, used in this work, is using hybrid scheme, by combining convenient numerical schemes. Two well known schemes are used in this paper, the Lax-Wendroff (LW) and the Lax-Friedrichs (LF) scheme. The first one is dispersive scheme, suffering from oscillations at discontinuities. The second one is a diffusive scheme, smoothing solution at discontinuities. The composite schemes [8, 11, 7] are a global composition of several steps of LW scheme followed by one step of the LF scheme. The diffusion is added by the LF scheme in the whole computational domain and the composite schemes remain only first order accurate as the LF scheme. Hybrid schemes investigated in this paper use an affine combination of the LW and LF numerical fluxes. The affine switch is designed in such a way that in regions of smooth solution only the LW numerical flux is used while the diffusive LF flux is used around discontinuities. In such a way hybrid schemes remain second order accurate on smooth solutions. Hybrid schemes have been originally developed on static Eulerian mesh with different switches [5, 4, 9]. Here we extend these ideas to Lagrangian formulation on computational mesh moving with the fluid.

The Euler equations express the conservation of the mass, momentum and total

---

\*This work was partly supported Czech Technical University internal Grant CTU0410914.

energy. The equations written in Lagrangian coordinates are

$$\rho \frac{d\vec{\omega}}{dt} + \nabla_{\vec{x}} \vec{f} = 0, \quad \vec{\omega} = \begin{pmatrix} \eta \\ \vec{v} \\ E \end{pmatrix}, \quad \vec{f} = \begin{pmatrix} \vec{v} \\ -pI \\ -p\vec{v} \end{pmatrix} \quad (1.1)$$

where  $\eta = 1/\rho$  is specific volume,  $\rho$  is density,  $\vec{v}$  is the velocity of the fluid,  $E$  is mass density of the total energy,  $p = p(\rho, e)$  is the pressure that is given by a state equation of fluid and  $I$  is the unit vector of the same dimension as the velocity. The equation of state for polytropic ideal gas  $p = (\gamma - 1) \frac{e}{\rho}$  is used. The movement of Lagrangian coordinates is controlled by the ordinary differential equation  $d\vec{x}/dt = \vec{v}$  which after discretization describe the movement of the computational mesh. The computational mesh is moving with the fluid, so the mass of computational cells remains constant. This basic Lagrangian assumption is often used for evaluation of density from the movement of the mesh.

**2. Lax-Wendroff and Lax-Friedrichs schemes in 1D.** Lax-Wendroff (LW) [6] and Lax-Friedrichs (LF) [3] are classical schemes for conservation laws. We use them in their two step form. The computational mesh is presented in Fig. 2.1 showing primary and dual cells. Vertices of the primary cells are drawn by full circles and denoted by indices  $k$ . Vertices of the dual mesh are drawn by empty circles, denoted by indices  $z$ . Primary cells are denoted by indices  $z$  and dual cells are denoted by indices  $k$ . Centers of cells, i.e. positions of vertices of dual cells, are computed as  $X_z = \frac{1}{2}(X_k + X_{k+1})$ ,  $X_k$  are the positions of primary vertices  $k$ .  $M_z$  denotes the mass of primary cell  $z$  and  $M_k$  mass of vertex  $k$ , i.e. the mass of dual cell  $k$ . All quantities are cell centered, i.e. defined inside the cell. The mass of primary cell  $M_z$  remains constant. The LF scheme in its two step form consists of a predictor and

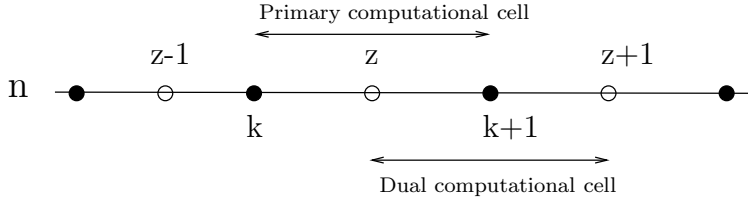


FIG. 2.1. Primary and dual cells, values discretized in cells.

corrector step, where the predictor step, computing the values on time level  $n + 1/2$  in the dual cell  $k$  has the form

$$\omega_k^{n+1/2} = \frac{M_{z-1}\omega_{z-1}^n + M_z\omega_z^n}{M_{z-1} + M_z} + \frac{\Delta t}{M_{z-1} + M_z} (f_z^n - f_{z-1}^n). \quad (2.1)$$

The upper index of the terms  $\omega$  and  $f$  denotes the time level. The corrector of the LF scheme computing values on time level  $n + 1$  using values on time level  $n + 1/2$  is

$$\omega_z^{n+1} = \frac{\omega_k^{n+1/2} + \omega_{k+1}^{n+1/2}}{2} + \frac{\Delta t}{2M_z} (f_{k+1}^{n+1/2} - f_k^{n+1/2}). \quad (2.2)$$

The LF scheme is diffusive and first order accurate. Its diffusion smears considerable the discontinuities.

The LW scheme in its two step form has the predictor identical to the predictor of the LF scheme (2.1). The LW corrector is

$$\omega_z^{n+1} = \omega_z^n + \frac{\Delta t}{M_z} \left( f_{k+1}^{n+1/2} - f_k^{n+1/2} \right). \quad (2.3)$$

The LW scheme is dispersive and second order accurate. The dispersion produces oscillations behind discontinuities.

The schemes are developed on the mesh which is moving with the fluid. The coordinates of primary nodes are not independent variables and are computed by using Euler method to solve the above mentioned ordinary differential equation in each node  $X_k^{n+1} = X_k^n + \Delta t v_k$ , where using chosen discretization the velocity  $v_k$  can be velocity on time level  $n+1/2$  or some linear interpolation of velocities on time levels  $n$ ,  $n+1/2$  and  $n+1$ . After moving the mesh, density as a function of the volume and the mass of the cells is computed  $\rho_z = M_z / (X_{k+1} - X_k)$  so, that the density corresponds exactly to the mesh motion. Other components of  $\omega$  are evaluated from the scheme (2.1), (2.2), and (2.3).

**3. Hybrid schemes in 1D.** The LF scheme is of the first order of accuracy and is excessively diffusive, while the LW scheme, although it is second order accurate, suffers from nonphysical oscillations, that appear behind the shocks. One approach how to deal with these undesirable properties is to use the so called composite LWLFn scheme. The idea of the composite LWLFn scheme is to use  $(n-1)$  steps of the LW scheme and once use the LF scheme as a consistent filter suppressing the LW oscillations. By using one step of the LF scheme, so called numerical diffusion is introduced into the computations [8]. For the composite schemes in Lagrangian coordinates see [11, 7]. Although the composite schemes work reasonably well, they include the first order numerical diffusion even in the areas of smooth solution and remain only first order accurate even on the smooth solution. The idea of hybrid schemes is to conveniently mix the LW and LF schemes locally in each cell and to introduce the numerical diffusion from the LF scheme only in the areas of discontinuity and to use only the second order LW scheme in smooth regions [5, 4, 9].

Both schemes can be written in the so called conservative form, when the value on the next time level  $(n+1)$  is expressed by the one-step form of the scheme as an addition of a difference of numerical fluxes over the edges of the cell  $z$  to the value on the time level  $n$ . The conservative form of each scheme  $S$ ,  $S \in \{LW, LF\}$  is

$$M_z \omega_z^{n+1} = M_z \omega_z^n + F_{k+1}^{(S)} - F_k^{(S)}, \quad (3.1)$$

The hybrid scheme combines the numerical flux  $F^{(S)}$  of the LW and LF scheme locally. For each node the affine combination of both fluxes given by parameter  $\alpha_k \in (0, 1)$

$$F_k^{(H)} = \alpha_k F_k^{(LF)} + (1 - \alpha_k) F_k^{(LW)}, \quad (3.2)$$

is used as the numerical flux of the hybrid scheme

$$M_z \omega_z^{n+1} = M_z \omega_z^n + F_{k+1}^{(H)} - F_k^{(H)}.$$

The parameter  $\alpha_k$  is a shock switch which should be close to one near discontinuous solution and close to zero in smooth regions. This means, that the switch is switching to the LF numerical fluxes and thus computational diffusion is added when discontinuity appears and in the areas with smooth solution, the flux of the LW scheme is

used. The shock switches due to Harten-Zwas [5], Harten [4], MacCormack-Baldwin [9] and Wendroff switch [1] have been modified for the non equidistant mesh.

The form (3.1) can be obtained by substituting the predictor terms into the corrector of the corresponding scheme and splitting the terms so that they form the numerical fluxes  $F_{k+1}^{(S)}$ . Our requirement on the numerical flux over the edge  $k+1$  is, that the form  $F_{k+1}$  has to be antisymmetric with respect to edge  $k+1$ . It means that when computing value  $\omega_z$ , we have to add to this value the same flux  $F_{k+1}$  as we subtract from the value in cell  $z+1$ .

The numerical fluxes of the LF scheme can be derived as

$$F_k^{(LF)} = \frac{1}{2} \left[ \frac{M_z M_{z-1} (\omega_z^n - \omega_{z-1}^n)}{M_z + M_{z-1}} + \Delta t \frac{M_{z-1} f_z}{M_z + M_{z-1}} + \Delta t \frac{M_z f_{z-1}}{M_z + M_{z-1}} + \Delta t f_k \right].$$

The LW corrector (2.3) is already in the conservative form and the LW numerical fluxes are  $F_k^{(LW)} = \Delta t f_k^{n+1/2}$ .

**4. Lax-Wendroff and Lax-Friedrichs schemes in 2D.** In 2D we use the quadrilateral mesh displayed in Fig. 4.1. Primary cells of the computational mesh are denoted by the pair of indices  $(i, j)$  and vertices by  $(i + 1/2, j + 1/2)$ . The values  $\omega_{(i,j)}^n$ , and  $f(\omega_{(i,j)}^n)$  denoted as  $f_{(i,j)}^n$  are discretized in the primary cells drawn by solid lines. The mass  $M_{(i,j)}$  of the primary cells is constant. Dual values at time level  $n + 1/2$  computed by the predictor are discretized in the dual cells, drawn by dashed lines. The dual cell's boundaries are created by connecting the centers of edges of primary cells with the primary cells centers, so that dual cells are 8-laterals. Dual edges divide each primary cell into four subzones which are denoted locally by (1) ... (4) counterclockwise starting by lower left subzone as shown in Fig. 4.1. The center of the primary cell is given by the average of its four vertices.

For periodicity in the local denotation (e.g. subzone (5) is subzone (1) or  $(-1)$  corresponds to (4)) we introduce the function  $rot : N \rightarrow \{1 \dots 4\}$  as

$$rot(n) = \begin{cases} (n) & \text{if } 0 < n \leq 4 \\ rot(n+4) & \text{if } n \leq 0 \\ rot(n-4) & \text{if } n > 4 \end{cases}$$

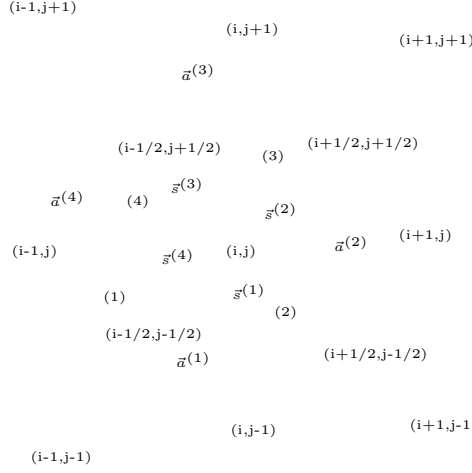
The vectors  $\vec{s}^{(1)} \dots \vec{s}^{(4)}$  are the normals to the abscissas connecting the center of primary cell and center of primary edge. Norms of those vectors are equal to lengths of these abscissas. The vector  $\vec{s}^{(n)}$  is normal of abscissa between subzone  $(n)$  and  $rot(n+1)$ . The vectors  $\vec{a}^{(1)} \dots \vec{a}^{(4)}$  are the normals to the edges of primary cell with size being equal to the length of the primary edge. Vectors are numbered counterclockwise, and  $\vec{a}^{(1)}$  is the normal to the bottom edge of the cell as shown in Fig. 4.1.

For shortening the formulas we define local shifting operators  $P_1 \dots P_4$

$$\begin{aligned} P_1(i, j) &= (i - 1/2, j - 1/2) & P_2(i, j) &= (i + 1/2, j - 1/2) \\ P_3(i, j) &= (i + 1/2, j + 1/2) & P_4(i, j) &= (i - 1/2, j + 1/2). \end{aligned}$$

The 2D LF predictor (which is 2D analog of 1D predictor (2.1)) is given by

$$\omega_a^{n+1/2} = \frac{1}{4M_a} \sum_{k=1}^4 M_{P_k(a)} \omega_{P_k(a)} + \frac{\Delta t}{2M_a} \sum_{k=1}^4 \vec{f}_{P_k(a)}^n \vec{S}_{P_k(a)}^{rot(k+2)}, \quad (4.1)$$


 FIG. 4.1. *Quadrilateral mesh*

where the index  $a$  denotes any dual cell  $(i + 1/2, j + 1/2)$ . The LF corrector is

$$\begin{aligned} \omega_b^{n+1} &= \frac{1}{4} \sum_{k=1}^4 \omega_{P_k(b)}^{n+1/2} + \frac{\Delta t}{2M_b} \sum_{k=1}^4 \bar{f}_{P_k(b)}^{n+1/2} \bar{A}_{P_k(b)}^{(k)} \\ \bar{A}^{(n)} &= \frac{1}{2} \left( \bar{a}^{(n)} + \bar{a}^{rot(n-1)} \right), \quad \bar{S}^{(n)} = \left( \bar{s}^{(n)} - \bar{s}^{rot(n-1)} \right), \end{aligned} \quad (4.2)$$

where the index  $b$  denotes any primary cell  $(i, j)$ . The predictor of the LW scheme is the same as the LF predictor. The corrector of LW scheme can be written as

$$\omega_b^{n+1} = \omega_b^n + \frac{\Delta t}{M_b} \sum_{k=1}^4 \bar{f}_b^{n+1/2} \bar{A}_{P_k(b)}^{(k)} \quad (4.3)$$

After computing of values on the time level  $n + 1$ , the new positions of the primary vertices have to be computed. For the mesh movement, we use the velocities  $\bar{v}_a^{n+1/2}$  obtained by the predictor. The positions of the primary vertices at time level  $n + 1$  are evaluated by  $\bar{X}_a^{n+1} = \bar{X}_a^n + \Delta t \bar{v}_a^{n+1/2}$ . The density of cells is computed from the mesh movement as  $\rho_b^{n+1} = V_b^{n+1}/M_b$ , where  $V_b^{n+1}$  is the volume of the cell  $b$ , while the other components of  $\omega$  are obtained from the schemes (4.1)-(4.3).

**5. Hybrid schemes in 2D.** For hybrid method both LF and LW schemes have to be written in the conservative form

$$M_{i,j} \omega_{i,j}^{n+1} = M_{i,j} \omega_{i,j}^n + F_{i+1/2,j} - F_{i-1/2,j} + F_{i,j+1/2} - F_{i,j-1/2}, \quad (5.1)$$

however to simplify the notation we work with the numerical fluxes  $\mathcal{F}$  defined locally in the cell  $(i, j)$  for which

$$M_{i,j} \omega_{i,j}^{n+1} = M_{i,j} \omega_{i,j}^n + \mathcal{F}_{i+1/2,j} + \mathcal{F}_{i,j+1/2} + \mathcal{F}_{i-1/2,j} + \mathcal{F}_{i,j-1/2}.$$

To obtain the LF scheme in its conservative form, the predictor (4.1) has to be substituted into the corrector (4.2). The derivation of the flux form is quite complicated, here we present only the results, the detailed description can be found in [1].

The numerical flux of the LF scheme splits into three parts

$$\begin{aligned}\mathcal{F}_{i+1/2,j} &= \mathcal{F}_{i+1/2,j}^\omega + \mathcal{F}_{i+1/2,j}^f + \mathcal{F}_{i+1/2,j}^{ff}, \\ \mathcal{F}_{i,j+1/2} &= \mathcal{F}_{i,j+1/2}^\omega + \mathcal{F}_{i,j+1/2}^f + \mathcal{F}_{i,j+1/2}^{ff},\end{aligned}$$

where  $\mathcal{F}^\omega$ ,  $\mathcal{F}^f$  and  $\mathcal{F}^{ff}$  are symbols for summation of terms containing  $\omega^n$ ,  $f^n = f(\omega^n)$  and  $f^{n+1/2} = f(\omega^{n+1/2})$ , respectively, given by

$$\begin{aligned}\mathcal{F}_{(i+1/2,j)}^\omega &= \sum_{k \in \{-1,1\}} Q_{(i+1/2,j+k/2)}^{[(i,j+k),(i+1,j)]} + Q_{(i+1/2,j+k/2)}^{[(i,j),(i+1,j+k)]} + 2Q_{(i+1/2,j+k/2)}^{[(i,j),(i+1,j)]} \\ \mathcal{F}_{(i,j+1/2)}^\omega &= \sum_{k \in \{-1,1\}} Q_{(i+k/2,j+1/2)}^{[(i+k,j),(i,j+1)]} + Q_{(i+k/2,j+1/2)}^{[(i,j),(i+k,j+1)]} + 2Q_{(i+k/2,j+1/2)}^{[(i,j),(i,j+1)]} \\ \mathcal{F}_{i+1/2,j}^f &= \sum_{k \in \{-1,1\}} R_{(i+1/2,j+k/2)}^{[(i,j+k),(i+1,j)]} + R_{(i+1/2,j+k/2)}^{[(i,j),(i+1,j+k)]} + 2R_{(i+1/2,j+k/2)}^{[(i,j),(i+1,j)]} \\ \mathcal{F}_{i,j+1/2}^f &= \sum_{k \in \{-1,1\}} R_{(i+k/2,j+1/2)}^{[(i+k,j),(i,j+1)]} + R_{(i+k/2,j+1/2)}^{[(i,j),(i+k,j+1)]} + 2R_{(i+k/2,j+1/2)}^{[(i,j),(i,j+1)]} \\ \mathcal{F}_{i+1/2,j}^{ff} &= \frac{\Delta t}{4} \left( \vec{f}_{(i+1/2,j-1/2)} \cdot \vec{A}_{(i,j)}^{(2)} + \vec{f}_{(i+1/2,j+1/2)} \cdot \vec{A}_{(i,j)}^{(3)} \right) \\ \mathcal{F}_{i,j+1/2}^{ff} &= \frac{\Delta t}{4} \left( \vec{f}_{(i+1/2,j+1/2)} \cdot \vec{A}_{(i,j)}^{(3)} + \vec{f}_{(i-1/2,j+1/2)} \cdot \vec{A}_{(i,j)}^{(4)} \right),\end{aligned}$$

where the forms  $Q$  and  $R$  are defined as

$$\begin{aligned}Q_d^{[A,B]} &= \frac{M_A M_B (\omega_B - \omega_A)}{32M_d}, \\ R_d^{[A,B]} &= \frac{M_A \vec{f}_B \cdot \vec{S}_B^{(n1)} - M_B \vec{f}_A \cdot \vec{S}_A^{(n2)}}{16M_d},\end{aligned}$$

where the superscripts of  $Q$  or  $R$  are the primary vertices and the subscript denotes the dual cell. The values  $n1$  and  $n2$  are not necessary to write, as they are uniquely determined by the arguments of  $R$ . The terms  $\mathcal{F}$  are defined locally with respect to the cell  $(i, j)$ , to keep the global definition of numerical fluxes (5.1), we define

$$\begin{aligned}F_{i+1/2,j}^{(LF)} &= \mathcal{F}_{i+1/2,j}, & F_{i-1/2,j}^{(LF)} &= -\mathcal{F}_{i-1/2,j} \\ F_{i,j+1/2}^{(LF)} &= \mathcal{F}_{i,j+1/2}, & F_{i,j-1/2}^{(LF)} &= -\mathcal{F}_{i,j-1/2}.\end{aligned}$$

For the Lax-Wendroff scheme, the flux decomposition can be found easily from (4.3),

$$\begin{aligned}F_{i+1/2,j}^{(LW)} &= \frac{\Delta t}{2} \vec{a}_{(i,j)}^{(2)} \cdot \left( \vec{f}_{(i+1/2,j-1/2)} + \vec{f}_{(i+1/2,j+1/2)} \right), \\ F_{i-1/2,j}^{(LW)} &= -\frac{\Delta t}{2} \vec{a}_{(i,j)}^{(4)} \cdot \left( \vec{f}_{(i-1/2,j+1/2)} + \vec{f}_{(i-1/2,j-1/2)} \right), \\ F_{i,j+1/2}^{(LW)} &= \frac{\Delta t}{2} \vec{a}_{(i,j)}^{(3)} \cdot \left( \vec{f}_{(i+1/2,j+1/2)} + \vec{f}_{(i-1/2,j+1/2)} \right), \\ F_{i,j-1/2}^{(LW)} &= -\frac{\Delta t}{2} \vec{a}_{(i,j)}^{(1)} \cdot \left( \vec{f}_{(i-1/2,j-1/2)} + \vec{f}_{(i+1/2,j-1/2)} \right).\end{aligned}$$

In 2D the shock switch is defined on each primary edge and the above numerical LF and LW fluxes are combined on each primary edge analogously as in (3.2) to obtain hybrid numerical fluxes.

**6. Numerical results.** The set of 1D Riemann problems described in Tab. 6.1 has been computed by different hybrid methods. The relative error

$$L_1 = \int_{\tilde{V}} |\rho^{(num)} - \rho^{(ex)}| / \int_{\tilde{V}} |\rho^{(ex)}|$$

of numerical solution is presented in Tab. 6.2. The value  $\rho^{(ex)}$  is the exact solution of Riemann problem and  $\rho^{(num)}$  is the numerical solution. The results are compared with the solution using shock switch  $\alpha = 0.2$  everywhere which is equivalent to the composite scheme LWLF5. The Fig. 6.1 presents results for the Riemann problem 4

Name	$\rho_L$	$u_L$	$p_L$	$\rho_R$	$u_R$	$p_R$	$x_0$	$T$
1	1	0.75	1	0.125	0	0.1	0.3	0.2
2	1	-2	0.4	1	2	0.4	0.5	0.15
3	1	-19.59745	1000	1	19.59745	0.01	0.8	0.012
4	5.99924	19.5975	460.894	5.999242	-6.19633	46.095	0.4	0.035
5	1.4	0	1	1	0	1	0.5	2
6	1.4	0.1	1	1	0.1	1	0.5	2
Noh	1	1	$10^{-6}$	1	-1	$10^{-6}$	0.5	1

TABLE 6.1

Initial conditions for 1D Riemann problems. The gas state values on the left side of the point  $x_0$  are  $\rho_L$ ,  $u_L$ , and  $p_L$ , and on the right side of the  $x_0$  are  $\rho_R$ ,  $u_L$  and  $p_R$ . The problem is computed till time  $T$ .

	$\alpha = 0.2$	Harten-Zwas	Harten	MacCormack-Baldwin	Wendroff
1	0.56	0.49	0.58	0.52	0.51
2	0.48	1.32	0.31	0.33	1.06
3	1.64	1.55	1.32	1.14	1.99
4	1.14	0.45	0.58	0.55	0.67
5	0.39	0.63	0.11	0.08	0.13
6	0.39	0.63	0.11	0.08	0.13
Noh	0.44	0.44	0.38	0.42	0.56

TABLE 6.2

Relative  $L_1$  error in % for Riemann problems defined in Tab. 6.1.

computed by constant switch  $\alpha = 0.2$  and MacCormack-Baldwin switch. The problem

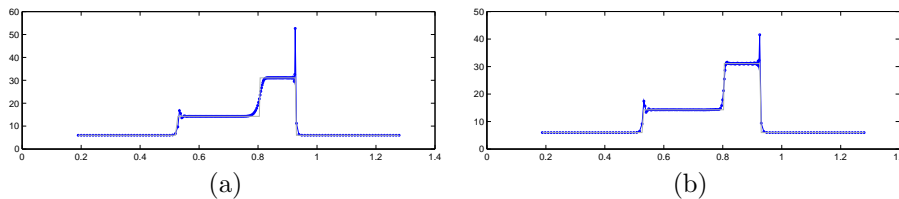


FIG. 6.1. Density for 1D Riemann problem 4 by (a): constant switch set to 0.2 (relative  $L_1$  error is 2.3%) and (b): MacCormack-Baldwin switch (relative  $L_1$  error is 1.4%). 200 cells.

with a smooth solution without a presence of discontinuities has been used to test the ability of the shock switches to detect a smooth solution and thus to use the LW scheme in these areas. Initial condition of the problem is  $\rho = 1 + 0.2 \sin(\pi x)$ ,

$v = 1$  and  $p = 1$ . The solution of this problem in time  $t$  is the density profile of  $\rho(t) = 1 + 0.2 \sin(\pi(x - tv))$ , other values are not changed. The problem has been computed till time  $t = 2.5$ . In Tab. 6.3 the convergence of composite and hybrid scheme is presented. The composite scheme is only first order while the hybrid scheme remains second order accurate.

	Number of cells	50	100	200	400	800
composite $\alpha = 0.2$	$L_1$ error [%]	3.2922	1.3717	0.6260	0.2997	0.1471
	$\log_2$	1.26	1.13	1.06	1.03	-
MacCormack- Baldwin switch	$L_1$ error [%]	0.0952	0.0263	0.0069	0.0017	0.0004
	$\log_2$	1.86	1.94	1.98	1.99	-

TABLE 6.3

*Convergence test of the smooth problem for composite and hybrid scheme.*

The Noh implosion problem with known exact solution was treated in 2D. The test simulates cylindrical implosion of a perfect gas with  $\gamma = 5/3$ , initial pressure is set to zero, density is equal to one, and velocity of magnitude equal to one with inward radial direction is set. Circular shock wave is generated at the center of convergence. Shock wave speed is equal to  $1/3$ . Behind the shock i.e. inside the circle, density is 16, the velocity is equal to zero and pressure  $p = 16/3$ . Ahead of shock wave, the gas is compressed because of convergence, which produces a density profile equal to  $\rho_{OUT} = 1 + t/\sqrt{(x^2 + y^2)}$ ,  $t$  is time, pressure and velocity remain the same as in initial conditions. Cartesian mesh with  $50 \times 50$  cells is used on upper right quadrant, symmetry boundary conditions are employed along the  $x$  and  $y$  axes. In Fig. 6.2 comparison of composite scheme LWLF5 and hybrid scheme with Harten-Zwas switch is presented. Decrease of overshoot on the head of shock by presence of the viscous term from the LF scheme is significant. In contrary, the computational mesh is more deformed when hybrid scheme is used.

Dukowicz problem is a two dimensional shock refraction problem. A vortex sheet is generated by the interaction of a shock with an inclined interface, and the mesh is uneven. The problem takes two adjacent regions of gas with different densities, with interface aligned at  $30^\circ$  to the horizontal. Gas with pressure  $p = 1$ ,  $\vec{v} = \vec{0}$  and  $\gamma = 1.4$  is considered. Initial mesh is presented in Fig. 6.3. Mesh is created by  $100 \times 50$  cells. First 50 columns in mesh covers left region of a computational domain with the density equal to one, next 50 columns cover the second region with  $\rho_2 = 1.5$ . A piston moves from the left with velocity 1.48, sending a shock ahead of it. Problem is run till the time  $t = 1.3$ . Comparison of uniformly set switch  $\alpha = 0.2$  and MacCormack-Baldwin switch is presented in Fig. 6.4. The boundaries of transmitted shock wave are sharper for hybrid method however some oscillations appear.

**7. Conclusion.** Hybrid methods for treating Euler equations in Lagrangian coordinates on a moving computational mesh have been developed and tested. In comparison to the composite LWLFn methods, the hybrid methods give generally comparable or better results. Hybrid methods are second order accurate while composite only first order. The disadvantage of the hybrid methods is, that the choice of convenient shock switch and its parameters is not straightforward and might need some tuning. The consequence of the local combination of two schemes is, that the computational mesh mostly suffers from bigger distortions than the composite LWLFn methods.



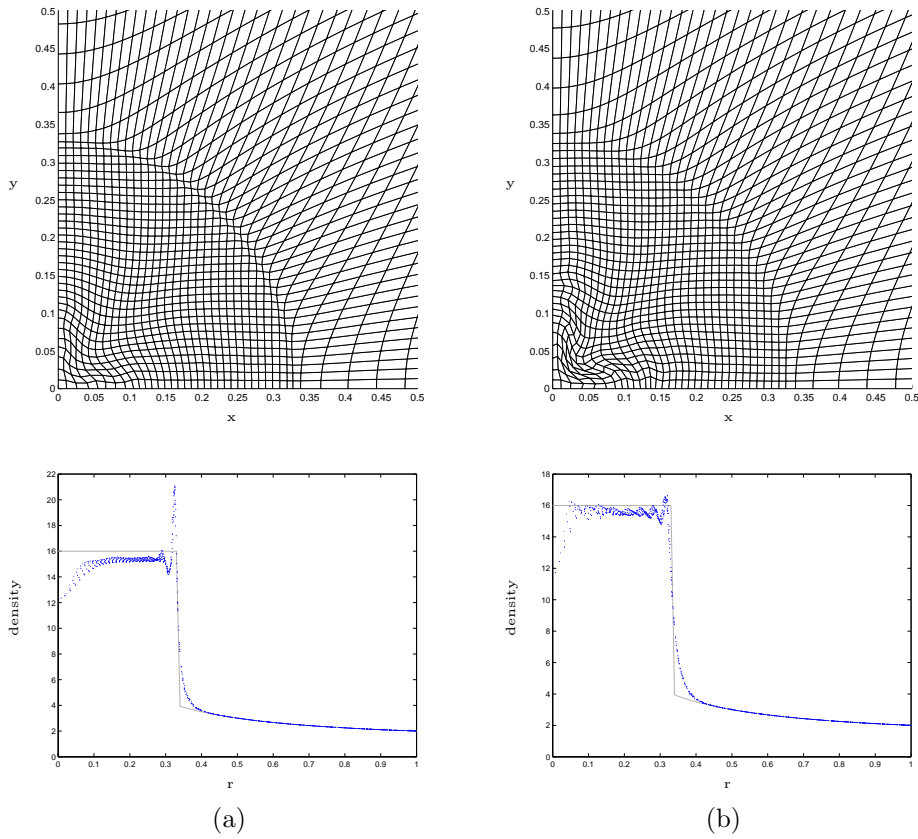


FIG. 6.2. Computational mesh and radial scatter plot profiles of density for 2D Noh problem at time  $t = 1$ , computed (a) by composite scheme LWLF5 (relative  $L_1$  error is 3.8%), (b) by hybrid method using Harten-Zwas switch (relative  $L_1$  error is 3.1%). Exact solution is displayed by the solid line.

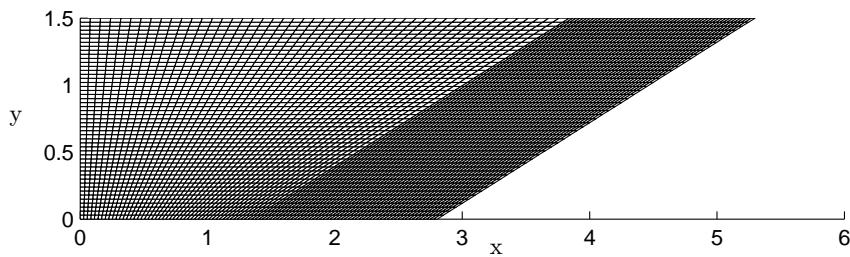


FIG. 6.3. Initial mesh configuration for Dukowicz problem.

**Acknowledgments.** The authors thank B. Wendroff for fruitful discussions and constructive comments.

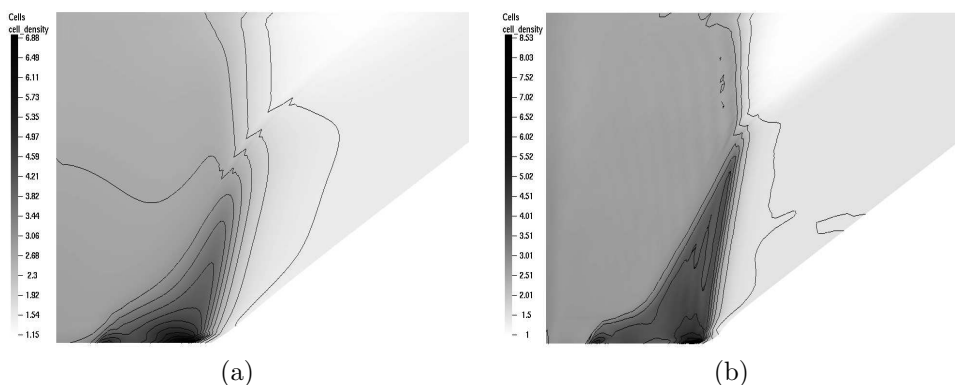


FIG. 6.4. Density of Dukowicz problem solution. (a): scheme computed by switch uniformly set to  $\alpha = 0.2$ , (b): MacCormack-Baldwin shock switch.

## REFERENCES

- [1] P. BUREŠ, *Hybrid schemes for Lagrangian methods*, Master's thesis, Czech Technical University, 2004.
- [2] E. CARAMANA, M. J. SHASHKOV, AND P. WHALEN, *Formulations of artificial viscosity for multi-dimensional shock wave computations*, J. Comp. Phys., 144 (1998), pp. 70–97.
- [3] K. FRIEDRICHS AND P. LAX, *System of conservation equations with a convex extension*, Proc. Nat. Acad. Sci., 68 (1971), pp. 1686–1688.
- [4] A. HARTEN, *The artificial compression method for computation of shocks and contact discontinuities: III self adjusting hybrid schemes*, Mathematics of Computation, 32 (1978), pp. 363–389.
- [5] A. HARTEN AND G. ZWAS, *Self-adjusting hybrid schemes for shock computations*, J. Comp. Phys., 6 (1972), pp. 568–583.
- [6] P. LAX AND B. WENDROFF, *Systems of conservation laws*, Comm. Pure Appl. Math., 13 (1960), pp. 217–237.
- [7] R. LISKA, M. SHASHKOV, AND B. WENDROFF, *Lagrangian composite schemes on triangular unstructured grids*, in Mathematical and Computer Modelling in Science and Engineering, International Conference in honour of the 80th birthday of K. Rektorys, M. Koandrlov and V. Kellar, eds., Prague, 2003, Union of Czech Mathematicians and Physicists, pp. 216–220.
- [8] R. LISKA AND B. WENDROFF, *Composite schemes for conservation laws*, SIAM J. Numer. Anal., 35 (1998), pp. 2250–2271.
- [9] R. W. MACCORMACK AND B. BALDWIN, *A numerical method for solving the Navier-Stokes equations with application to shock-boundary layer interactions*, Tech. Rep. 75-1, AIAA, 1975.
- [10] M. SHASHKOV, *Conservative Finite-Difference Methods on General Grids*, CRC Press, Boca Raton, Florida, 1996.
- [11] M. SHASHKOV AND B. WENDROFF, *A composite scheme for gas dynamics in Lagrangian coordinates*, J. Comp. Phys., 150 (1999), pp. 502–517.